DROP-SCALE NUMERICAL MODELING OF CHEMICAL PARTITIOING DURING CLOUD HYDROMETEOR FREEZING

A.L. Stuart[1] and M.Z. Jacobsonr[2]

[1]Department of Atmospheric Sciences, Texas A&M University, College Station, TX, 77843, USA
[2]Department of Civil and Environmental Engineering, Stanford University, Stanford, CA, 94305, USA

1. INTRODUCTION

Thunderstorms can significantly impact chemical distributions in the troposphere by 1) redistribution of air and hydrometeors containing trace chemicals and 2) providing a multi-phase environment for chemical phase changes and reactions. Interactions between ice-containing hydrometeors and chemicals are not well understood. Laboratory and field measurements of chemical partitioning during drop freezing provide greatly varying estimates of the retention efficiency of volatile solutes (e.g., Lamb and Blumenstein, 1987; Iribarne and Pyshov, 1990, Snider and Huang, 1998; Voisin and Legrand, 2000). Our recent work using a theory based time scales analysis to calculate the retention efficiency provided a basic understanding of the dependence of partitioning on chemical properties and freezing conditions (Stuart and Jacobson, 2003, 2004). In this work, we develop a drop-scale time-dependent numerical model of drop freezing and chemical transfer to investigate the effects on chemical partitioning of dynamical interactions between involved processes.

2. MODEL DESCRIPTION

Our one-dimensional (radial) model represents the freezing of a spherical solute-containing liquid hydrometeor with a riming substrate or ice nuclei at its center. Processes represented by the model include radial inter- and intra-phase heat and mass transfer, freezing kinetics, latent heat release during freezing, and solute segregation and trapping at the freezing interface.

2.1 Process Representation

The model is initiated at freezing nucleation. As time progresses, the drop freezes and solute is expelled at rates governed by both the grid-resolved partial differential equations for radial heat and mass transfer as well as the sub-grid scale differential equations for processes occurring near the ice water interface. We represent the multi-phase (dendritic) character of freezing in the super-cooled drop using average water and ice amounts (fractions) in each radial shell

Corresponding author's address: Dr. Amy L. Stuart, Dept. of Atmospheric Sciences, Texas A&M University, 3150 TAMU, College Station, TX 77843-3150; E-Mail: amystuart@tamu.edu.

volume. Properties and prognostic variables (temperatures and solute concentrations) are also volume average values for each phase. This 'mushy zone' representation (after Tien and Geiger, 1967) of the non-planar ice-water interface assumes phase changes (freezing) provide a volume source of latent heat. The density of water and ice is assumed to be constant and equivalent in both phases.

Processes resolved on the model grid include radial intra- and inter-phase heat and mass transfer. Equations for diffusive transfer for each phase were derived using energy and mass balances over a shell. Inter-phase transfer coefficients were based on two-film theory (e.g. Sherwood et al., 1975) and account for mass transfer resistances in both phases. Boundary conditions at the grid's outer boundary (the hydrometeor surface) account for flux due to conduction, evaporation, sublimation, and condensation. Flux enhancement due to fluid flow around the hydrometeor is represented with a flow-dependent ventilation coefficient.

Processes represented at the sub-grid scale include phase change, latent heat transfer, inter-phase heat transfer, and solute mass segregation during phase change. Rates of freezing (and melting) are represented by a kinetic equation for the interfacial growth velocity, which is based on theory and experimental data on growth rates of ice in super-cooled water (Bolling and Tiller, 1961; Pruppacher and Klett, 1997). We estimate the interfacial surface area as the ratio of the shell surface area to its volume. To simulate dendrite-like growth, ice initiation in any cell can only occur if an adjacent shell contains ice. To represent latent heat transfer, we perform an enthalpy balance over the grid shell. Energy distribution to each phase is weighted by the volume fraction of each phase in a shell. For phase initiation in a given shell, we assume the temperature in both phases remains equal. Inter-phase heat flux is represented as conductive transfer for which the bulk heat transfer coefficient is a function of the two-film inter-phase transfer coefficient and the dendrite tip radius. We assume free dendritic crystal growth and calculate the dendrite tip radius as a function of the dendrite Peclet number and the interfacial growth velocity (after Caroli and Muller-Krumbhaar, 1995, and Libbrecht and Tanusheva, 1999). Solute mass segregation during freezing is calculated to maintain a mass balance, assuming equilibrium partitioning at the ice-water

interface. During melting, all mass in the melted ice is assumed to be transferred to the water phase. Trapping of concentrated solute between dendrite branches, leading to bulk non-equilibrium partitioning to ice, is represented by allowing grid shells that freeze completely in a given time step to retain all solute originally in that shell.

2.2 Flow of calculations and numerics

The flow diagram for model calculations is provided in Figure 1. The model is initiated by specifying ambient conditions (constant temperature and pressure), hydrometeor conditions (initial drop and ice substrate sizes, temperatures, and speed in air), initial solute concentrations in all phases, the outer-model time-step (used for grid-resolved processes), and the number of radial grid shells. The grid is determined and initialized with these inputs, assuming the drop water is spread evenly around the ice substrate. Following initialization, the model time cycle of processes begins. For each outer-model time-step, sub-grid processes of phase change with latent heat transfer, inter-phase heat transfer, and solute segregation and trapping are first calculated. Each process is calculated separately in a serial manner (i.e. processes are time-split). Phase change with latent heat transfer and inter-phase heat transfer calculations use an adaptive time-step to ensure physically-consistent results (e.g., temperatures at the interface that do no significantly overshoot the equilibrium freezing temperature). The grid-resolved processes of radial heat and mass transfer are then calculated for the outer-model time-step. A finite volume 2nd-order central difference discretization is used for calculation of radial fluxes. Progression in time is discretized with a Forward Euler formulation. After each outer-model time-step, values of system enthalpy and mass (of water and solute) are calculated to track conservation properties of the simulation. The model is terminated when the hydrometeor is completely frozen.

3. MODEL DEMONSTRATION

To test and demonstrate the model, we have applied it to simulate several cases of freezing of drops of varied sizes and ambient conditions. We will detail results for one demonstration case here and then briefly discuss model performance for all cases.

3.1 Case Description

Our demonstration case simulated the freezing of a hydrometeor falling at its terminal fall speed, formed due to the impaction of a supercooled drop (1000 μm in radius) with a ice substrate (100 μm in radius). The air and initial supercooled drop temperatures were –10°C. The initial ice substrate temperature was –5°C. The ambient pressure was 300 mbar. For demonstration, we used a hypothetical chemical
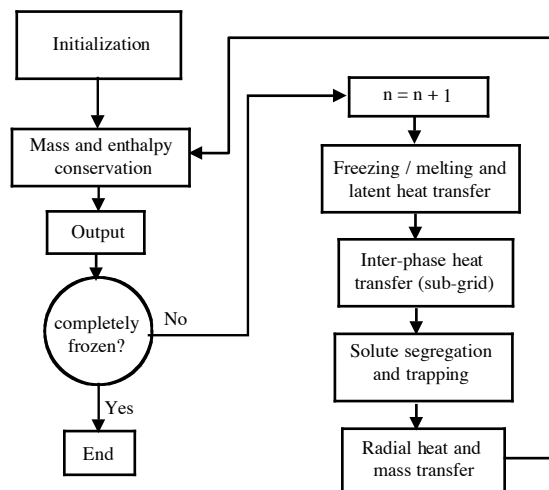
Figure 1. Flow diagram of model calculations, where n is the outer-model time-step.

solute with the following properties: dimensionless (concentration) Henry's constant of approximately 30, ice-water partition coefficient of 0, and diffusivities in air, water, and ice of 0.1 cm^2/s, 1x10^{-5} cm^2/s, and 1x10^{-10} cm^2/s, respectively. Solute concentrations in the gas phase and supercooled drop where initially at equilibrium, with values of 7x10^{-7} g/cm^3 and 2x10^{-5} g/cm^3, respectively. Initial solute concentration in the ice substrate was 0. The number of radial grid shells was specified as 10 and the outer-model time-step was 1x10^{-4} s.

3.2 Case Results

We will first describe the freezing progression and temperature changes in the hydrometeor. The hydrometeor is initially liquid throughout most of its radius, with a solid core (the original ice substrate). Ice quickly propagates out from the ice core, reaching the hydrometeor surface by 9x10^{-4} s. Ice fraction values throughout the mixed-phase region remain below 0.1 during this time. Water and ice temperatures in the mixed-phase region also increase from the inside of the hydrometeor outward (due to release of latent heat of freezing). Temperatures reach an approximately uniform value slightly below 273 K by 2x10^{-3} s. Once the mixed-phase region temperatures are approximately equivalent, the temperatures and ice fractions increase more slowly and uniformly. By approximately 4x10^{-3} s, we see the ice fraction near the air boundary surpass that in the hydrometeor interior. The temperature in the solid core (the original ice substrate) increases slowly (due to radial heat transfer from the mixed-phase zone), but does not reach the temperature of that zone until about 3x10^{-2} s. Far from the air boundary, the temperatures reach the equilibrium freezing temperature of water at approximately 0.1 s.

Temperatures near the air boundary are depressed (due to heat loss to air that is 263 K). By 7 seconds, an ice-shell (ice fraction of 1.0) has formed at the hydrometeor surface. Freezing propagates inward until the entire hydrometeor is frozen by 24.6 s. Temperatures (of ice) also decrease from the outside inward after the freezing front.

This progression of freezing and temperature change can be compared with experimental and theoretical studies of drop freezing (e.g. see Macklin and Payne, 1967, 1968; Griggs and Choularton, 1983; Pruppacher and Klett, 1997). These studies suggest that nucleated drops freeze in approximately two stages. The first stage is termed the adiabatic stage. During this stage, ice propagates out from the nucleation site and the drop heats up to the equilibrium freezing temperature of water, with relatively little heat loss to the drop environment. (This is termed the adiabatic stage.) This stage is very quick, orders of magnitude faster than the complete freezing of the drop. The second stage is termed the diabatic stage. During this stage the freezing occurs more slowly, limited by the rate of heat loss to the ice substrate and the surrounding air. This picture of freezing progression is qualitatively consistent with our results.

For quantitative comparison, we estimate the adiabatic freezing stage during our simulation to be within an order of magnitude of 0.01 s. (Bounded by the time it takes for ice to reach the drop surface, approximately 0.001 s, and the time it takes the mixed-phase zone to heat to approximately the equilibrium freezing temperature, 0.1 s). During this time, approximately 13% of the drop mass froze in our simulation. This is in excellent agreement to the value, $c_w \Delta T / L_m$ (or 13%), derived from drop freezing theory (Pruppacher and Klett, 1997). The complete drop freezing time from our simulation, 24.6 s, can also be compared to the bulk theoretical expression developed for drops falling freely in air (Pruppacher and Klett, 1997). This expression yields a value of 19.4 s for our simulated conditions, which is about 21% lower than our simulated value.

The progression of solute redistribution during freezing was also simulated. Solute concentrations in liquid water were initially 2.0×10^{-5} g/cm^3 throughout the hydrometeor and 0 in the ice core. As ice propagates outward, solute concentrations in water away from the air boundary increase slightly to 2.3×10^{-5} g/cm^3 at 1 s, due to the exclusion of solute from the ice phase during freezing. Concentrations near the air boundary decrease to 1.9×10^{-5} g/cm^3 at 1 s, due to mass transfer to air. After the outer shell of the hydrometeor freezes, and freezing propagates inward, concentrations in water near the inner boundary of the shell increase more dramatically to about 1×10^{-4} g/cm^3 due to exclusion from the ice phase and lack of a sink to air. In ice, average concentrations within and near the original ice core

jump to 7.0×10^{-9} g/cm^3 directly after freezing initiation, due to freeze trapping. As ice propagates through the hydrometeor, solute concentrations in ice increase to non-zero values, due to radial mass transfer. When the outer shell of the hydrometeor freezes, the concentration in ice near the air boundary jumps to 9.4×10^{-8} g/cm^3, also due to freeze trapping. As freezing progresses inward, higher concentrations are trapped in ice due to higher concentrations in the liquid. The final solute concentration profile indicates increasing solute concentrations inward, with the area near the hydrometeor surface (air boundary) having very low concentrations (approximately 1×10^{-7} g/cm^3) and the area frozen last (near the original ice core) having a concentration slightly higher that that originally in water (2.3×10^{-5} g/cm^3). The total retention efficiency in the hydrometeor (the ratio of the mass of solute in the hydrometeor to that originally in the drop) decreases precipitously from 1.0 to 0.96 in the first 0.1 s of freezing. It continues to decrease more slowly until an ice shell forms at the surface (at about 7 s). After ice shell formation, there is negligible loss and the retention fraction remains constant at 0.72. These results are qualitatively physical and consistent with the body of literature on crystallization separation (e.g. Zief and Wilcox, 1967). However, they cannot be quantitatively compared to experimental results due to our use of a hypothetical solute for demonstration.

3.3 Model Performance

For all cases simulated, freezing and solute redistribution occurred in a similar manner. Quantitative comparison of simulated freezing times to theoretical bulk estimates of freezing times yielded values in reasonable agreement (differences within approximately 20%). Mass and heat conservation was excellent for all case simulations, with exact solute and water mass balance and a very small (insignificant) heat balance error.

4. CONCLUSIONS

We have developed and demonstrated a one-dimensional radial model of chemical partitioning during hydrometeor freezing. Model results are physically consistent with freezing, heat, and mass transfer theory. The model is exactly mass conserving and also shows good energy conservation. Insights provided by results from model demonstration cases include that the location of nucleation within the drop may not be very important to overall drop freezing. Due to fast dendritic growth, the freezing front quickly moves to the drop surface and overall freezing progresses inward from the surface. Trapping due to ice shell formation at the hydrometeor surface may also play a large role in non-equilibrium bulk solute partitioning to the ice phase hydrometeor. Further development of the model will include 1) improvement of the dendrite initiation representation to account for the distance of tip travel, 2) improvement of the solute trapping representation through use of an effective ice-

liquid distribution coefficient dependent on the freezing rate and/or dendrite characteristics, 3) detailed testing of the freezing and chemical mass transfer modules, and 4) addition of a chemical reaction solver. We plan to apply the model to investigate the dynamics of chemical partitioning and reaction during freezing and riming in clouds. Results from these investigations will inform modeling and understanding of chemical scavenging and redistribution by clouds.

5. REFERENCES

Bolling, G. F. and W. A. Tiller, 1961: Growth from the Melt. III. Dendritic Growth. *Journal of Applied Physics*, **32,** 2587-2605.

Caroli, B. and H. Muller-Krumbhaar, 1995: Recent advances in the theory of free dendritic growth. *ISIJ International*, **35,** 1541-1550.

Griggs, D. J. and T. W. Choularton, 1983: Freezing modes of riming droplets with application to ice splinter production. *Quarterly Journal of the Royal Meteorological Society*, **109,** 243-253.

Iribarne, J. V. and T. Pyshnov, 1990: The effect of freezing on the composition of supercooled droplets - I. Retention of HCl, HNO_3, NH_3, and H_2O_2. *Atmospheric Environment*, **24A,** 383-387.

Lamb, D. and R. Blumenstein, 1987: Measurement of the entrapment of sulfur dioxide by rime ice. *Atmospheric Environment*, **21,** 1765-1772.

Libbrecht, K. G. and V. M. Tanusheva, 1999: Cloud chambers and crystal growth: effects of electrically enhanced diffusion on dendrite formation from neutral molecules. *Physical Review E*, **59,** 3253-3261.

Macklin, W. C. and G. S. Payne, 1967: A theoretical study of the ice accretion process. *Quarterly Journal of the Royal Meteorological Society*, **93,** 195-213.

Macklin, W. C. and G. S. Payne, 1968: Some aspects of the accretion process. *Quarterly Journal of the Royal Meteorological Society*, **94,** 167-175.

Pruppacher, H. R. and J. D. Klett, 1997: *Microphysics of Clouds and Precipitation*. 2nd ed. Vol. 18, Kluwer Academic Publishers, 954 pp.

Sherwood, T. K., R. L. Pigford, and C. R. Wilke, 1975: *Mass Transfer*. McGraw-Hill Book Company.

Snider, J. R. and J. Huang, 1998: Factors influencing the retention of hydrogen peroxide and molecular oxygen in rime ice. *Journal of Geophysical Research*, **103,** 1405-1415.

Stuart, A. L. and M. Z. Jacobson, 2003: A timescale investigation of volatile chemical retention during hydrometeor freezing: Nonrime freezing and dry growth riming without spreading. *Journal of Geophysical Research*, **108,** 4178, doi:10.1029/2001JD001408.

Stuart, A. L. and M. Z. Jacobson, 2004: Chemical retention during dry growth riming. Accepted for publication in *Journal of Geophysical Research*.

Tien, R. H. and G. E. Geiger, 1967: A heat-transfer analysis of the solidification of a binary eutectic system. *Journal of Heat Transfer*, **89,** 230-234.

Voisin, D. and M. Legrand, 2000: Scavenging of acidic gases (HCOOH, CH_3COOH, HNO_3, HCl, and SO_2) and ammonia in mixed liquid-solid water clouds at the Puy de Dome mountain (France). *Journal of Geophysical Research*, **105,** 6817-6835.

Zief, M. and W. R. Wilcox, 1967: *Fractional Solidification*. Vol. 1, Marcel Dekker, Inc, 714 pp.